Received: 14 February 2019 | Revised: 16 July 2019 | Accepted: 18 July 2019

DOI: 10.1111/pce.13625

ORIGINAL ARTICLE

WILEY Plant, Cell & Environment

Carbon isotopic tracing of sugars throughout whole-trees exposed to climate warming

Morgan E. Furze[1] | John E. Drake[2] | Julia Wiesenbauer[3] | Andreas Richter[3] | Elise Pendall[4]

[1] Department of Organismic and Evolutionary Biology, Harvard University, Cambridge, Massachusetts 02138

[2] Department of Forest and Natural Resources Management, College of Environmental Science and Forestry, State University of New York, Syracuse, New York 13210

[3] Department of Microbiology and Ecosystem Science, University of Vienna, Vienna 1010, Austria

[4] Hawkesbury Institute for the Environment, Western Sydney University, Penrith, New South Wales 2751, Australia

Correspondence
Morgan E. Furze, Department of Organismic and Evolutionary Biology, Harvard University, 26 Oxford St. Cambridge, MA.
Email: mfurze@fas.harvard.edu

Abstract

Trees allocate C from sources to sinks by way of a series of processes involving carbohydrate transport and utilization. Yet these dynamics are not well characterized in trees, and it is unclear how these dynamics will respond to a warmer world. Here, we conducted a warming and pulse-chase experiment on *Eucalyptus parramattensis* growing in a whole-tree chamber system to test whether warming impacts carbon allocation by increasing the speed of carbohydrate dynamics. We pulse-labelled large (6-m tall) trees with ^{13}C-CO_2 to follow recently fixed C through different organs by using compound-specific isotope analysis of sugars. We then compared concentrations and mean residence times of individual sugars between ambient and warmed (+3°C) treatments. Trees dynamically allocated ^{13}C-labelled sugars throughout the aboveground-belowground continuum. We did not, however, find a significant treatment effect on C dynamics, as sugar concentrations and mean residence times were not altered by warming. From the canopy to the root system, ^{13}C enrichment of sugars decreased, and mean residence times increased, reflecting dilution and mixing of recent photoassimilates with older reserves along the transport pathway. Our results suggest that a locally endemic eucalypt was seemingly able to adjust its physiology to warming representative of future temperature predictions for Australia.

KEYWORDS

carbon allocation, compound-specific isotope analysis, *Eucalyptus parramattensis*, heat, storage carbohydrates

1 | INTRODUCTION

Carbon (C) dynamics in trees result from the complex integration of multiple sinks competing for photoassimiliates supplied by sources (Kozlowski, 1992). As the C requirements of different organs and processes vary temporally due to normal functioning or unexpected stress, trees must adjust C allocation to survive. In general, a fraction of photoassimilates produced during photosynthesis in the leaves is exported into the phloem and allocated throughout the tree. The transport of photoassimilates from sources to sinks via the phloem is driven by a hydrostatic pressure gradient, which is controlled in part by the utilization of carbohydrates in sink organs (Knoblauch et al., 2016; Münch, 1930). Thus, along the long-distance transport pathway, photoassimilates are frequently exchanged with older reserves (i.e., nonstructural carbohydrates) and released into sinks to serve as C skeletons for growth, metabolism, and storage (reviewed in Furze, Trumbore, & Hartmann, 2018).

Environmental conditions have the potential to alter whole-tree C dynamics by influencing the activity of sources and sinks, with implications for ecosystem-level C budgets. For instance, temperature is likely to affect the rate of chemical reactions involved in carbohydrate utilization and in turn influence the distribution of carbohydrates throughout the tree. Elevated temperatures may increase sink strength (i.e., increased growth, respiration, and root exudation), leading to faster turnover rates of reserves in organs and faster transfer of sugars along the transport pathway (i.e., stimulation of phloem transport; Plain et al., 2009; Dannoura et al., 2011). Given that unprecedented temperature increases are expected across the globe, it is important to understand how within-tree C dynamics will respond to higher temperatures.

While some tree species adjust their physiology to changes in temperature (Reich et al., 2016), there is uncertainty surrounding the capacity for acclimation (Atkin & Tjoelker, 2003). Many studies have quantified physiological acclimation of photosynthesis and respiration to experimental warming (Aspinwall et al., 2016; Drake et al., 2016; Slot & Kitajima, 2015; Yamori, Hikosaka, & Way, 2014), but relatively few studies have quantified how experimental warming alters within-tree C dynamics associated with carbohydrate transport (Epron et al., 2012). That is, although previous studies have quantified physiological acclimation at the point of C uptake via photosynthesis and C release via respiration, the dynamics of internal carbohydrate transport that connect these endpoints of metabolism remains poorly studied. In the absence of a physiological change, warming is expected to increase carbohydrate utilization and thus transport, leading to a reduction in the concentrations and mean residence times (MRTs) of sugars throughout the tree.

Pulse-labelling with stable C isotopes has proven to be a valuable tool for understanding C dynamics, as it allows labelled carbon dioxide (CO_2) to be traced throughout plants (reviewed in Epron et al., 2012). In particular, ^{13}C-CO_2 pulse-chase experiments have been widely used to assess the temporal dynamics of labelled photoassimilates in trees growing in both natural (Kagawa, Sugimoto, & Maximov, 2006a) and perturbed conditions such as drought, increased temperature, and elevated CO_2 (Blessing, Werner, Siegwolf, & Buchmann, 2015; Hesse, Goisser, Hartmann, & Grams, 2018; Streit et al., 2013). However, previous studies have often used potted saplings or small trees (Barthel et al., 2011; Endrulat, Saurer, Buchmann, & Brunner, 2010; Vizoso et al., 2008), and individual branches or the crown (Epron et al., 2011; Kagawa, Sugimoto, & Maximov, 2006b; Plain et al., 2009). Few ^{13}C labelling experiments have been conducted on large whole-trees in the field (Epron et al., 2015; Kuptz, Fleischmann, Matyssek, & Grams, 2011; Warren et al., 2012). To our knowledge, only a single ^{13}C labelling experiment has been combined with longer-term warming, and this work was conducted on potted saplings (Blessing et al., 2015). Many aspects of tree morphology and physiology change as trees transition from small seedlings to large trees, including wood quantity, leaf mass fraction, and growth rates (Duursma & Falster, 2016; Poorter et al., 2012). Thus, how rising temperatures may affect the dynamics of carbohydrate transport and metabolism in large field-grown trees deserves attention.

Furthermore, processes involving C vary spatially within a tree, seasonally throughout the year, and on timescales ranging from minutes to decades, and different sugars serve specialized functions and may differentially respond to environmental change. For example, whereas sucrose and raffinose function as the main transport sugars, glucose and fructose play a large role in metabolism and osmoregulation (reviewed in Hartmann & Trumbore, 2016). The fate of the ^{13}C label can be tracked in the C of individual sugars using compound-specific isotope analysis (Richter et al., 2009). Thus, coupling compound-specific ^{13}C analysis of individual sugars with pulse labelling (Keel et al., 2012; Streit et al., 2013) allows higher resolution of whole-tree C dynamics, as they together capture the diverse exchanges between older reserves and newly fixed ^{13}C-labelled photoassimilates.

We conducted a warming and *in situ* ^{13}C-CO_2 pulse-chase experiment on whole-trees (Figure 1). Following pulse-labelling, leaves, phloem, and roots were collected for the measurement of sugar concentrations as well as the carbon isotope composition ($\delta^{13}C$) of sugars and bulk tissues using compound-specific isotope analysis. We hypothesized that warming would increase sink activity, resulting in reduced MRTs and reduced concentrations of sugars across organs. Our results provide insight into the physiological and environmental controls on whole-tree C source-sink relations, which has implications for tree and ecosystem function under global change.

2 | MATERIALS AND METHODS

2.1 | Study site

Our warming and ^{13}C-CO_2 pulse-chase experiment was conducted in a system of 12 whole-tree chambers (WTCs) located in Richmond, New South Wales, Australia (33°36′40″S, 150°44′26.5″E). This site has a mean annual temperature and mean annual precipitation of 17°C and 730 mm, respectively (1992–2014, Bureau of Meteorology, station 067105, ~ 5 km away). We selected six cylindrical chambers (~53 m^3) for this study, each enclosing a single tree of the locally endemic woodland tree species *Eucalyptus parramattensis* (Parramatta red gum). The WTCs monitored and controlled environmental parameters such as air temperature, vapour pressure deficit, and atmosphere CO_2 concentration and were subdivided with a suspended plastic floor sealed around the tree stem at 45 cm height to prevent the mixing of belowground and aboveground gas fluxes. The design and function of the WTCs have been previously described (Barton et al., 2010; Drake et al., 2016), including for this specific experiment with *E. parramattensis* (Drake et al., 2019).

2.2 | Warming and ^{13}C-CO_2 pulse-chase experiment

Potted seedlings that were germinated from seeds obtained from Harvest Seeds and Native Plants (Terry Hills, NSW, Australia) were placed into each WTC on October 28, 2015, and the experimental warming

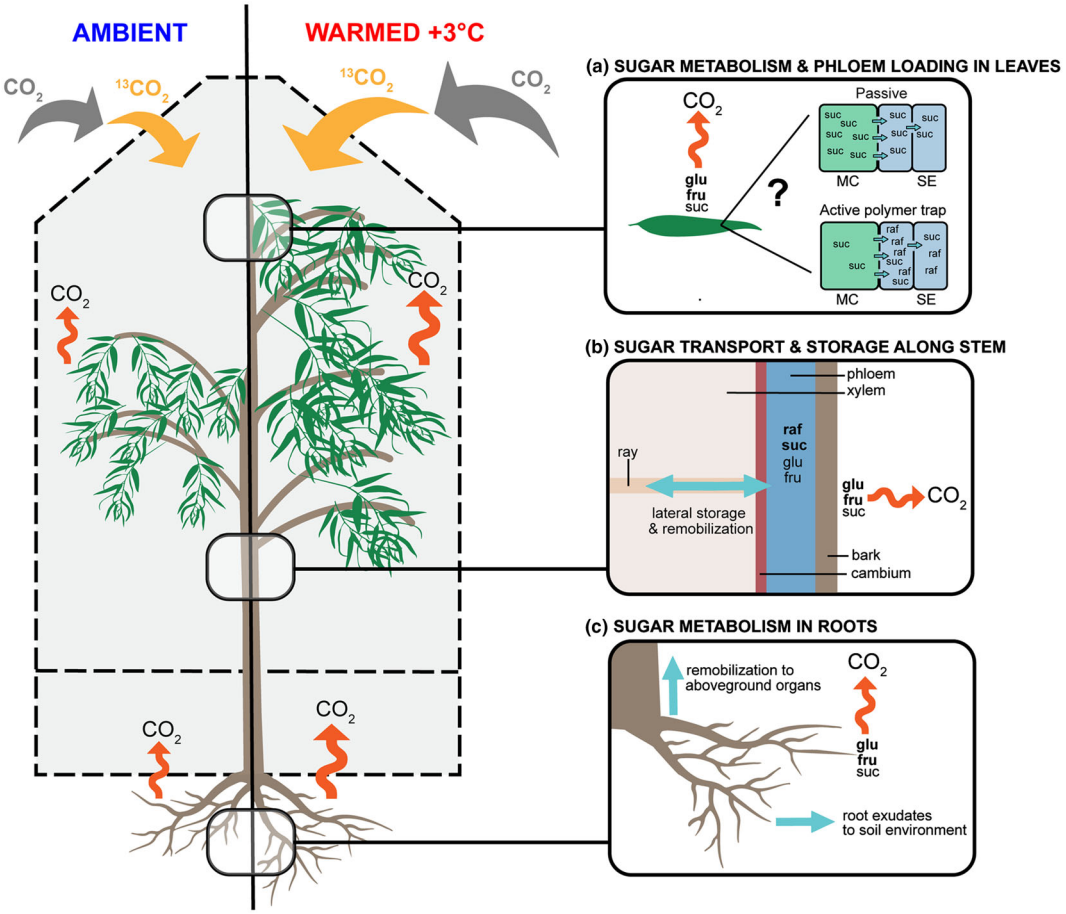

FIGURE 1 Comparison between *E. parramattensis* in whole-tree chambers growing under ambient and warmed (+3°C) treatments. Left: Trees grown in ambient conditions were smaller than those in warmed conditions and assimilated less ^{13}C-labelled CO_2 (yellow arrows). After the 4-hr labelling period, unlabelled CO_2 (grey arrows) was taken up and began to dilute the labelled C pool. We hypothesized that warming would increase sink activity compared to ambient conditions (i.e., respiration; orange wavy arrows), resulting in reduced concentrations and reduced mean residence times of soluble sugars throughout trees. Right: zoom-in overview of carbohydrate transport and utilization. (a) At the leaf level, sugars are quickly exported or respired. Glucose and fructose function as metabolites, whereas sucrose and raffinose serve as transport sugars and are loaded into the phloem and shuttled throughout the tree. There are three phloem loading mechanisms, two symplastic strategies (shown), and one apoplastic strategy (not shown). (b) Along the stem, sugars are used for biomass production, but they are also respired or stored. Older stem reserves are remobilized back into the phloem. Because the phloem is leaky, sugars are leaked out of and retrieved back into the phloem along the vertical long-distance transport pathway, leading to dilution of the ^{13}C label from the canopy to the roots. (c) Once at the roots, sugars are used for biomass production, stored, respired, or exuded to the soil environment. Older reserves are remobilized and transported back up to aboveground organs. Abbreviations: glu, glucose; fru, fructose; suc, sucrose; raf, raffinose; MC, mesophyll cell; SE, sieve element. Bolded sugars indicate dominant ones involved in the process depicted [Colour figure can be viewed at wileyonlinelibrary.com]

treatment was initiated. On December 23, 2015, one seedling was planted directly into the soil within each WTC. A belowground ~1m vertical root-exclusion barrier restricted the rooting volume of each tree. The long-term experimental warming treatment was previously described in Drake et al. (2018, 2019). In brief, the climate-controlled WTCs were evenly divided between ambient and warmed treatments (n = 6 trees per treatment). Ambient WTCs tracked relative humidity and air temperature of the study site, whereas warmed WTCs tracked ambient relative humidity and air temperature +3°C. The average warming was +2.9°C (±0.6 SD across 265 days) in the aboveground airspace, +2.6°C (±0.6) in the belowground airspace, +2.9°C (±0.8) for soil temperature at 5-cm depth, +3.0°C (±0.5) at 10-cm depth, +2.4°C (±0.2) at 20-cm depth, +1.7°C (±0.3) at 30-cm depth, and +1.6°C (±0.2) at 50-cm depth (Drake et al., 2019). An increase of 3°C is projected for Australia by 2100 (Australian Bureau of Meteorology State of the Climate Report, 2016; IPCC, 2014). Additionally, WTCs were irrigated every 2 weeks with half of the mean monthly rainfall measured over the past 30 years (Figure S1).

Nine months after the warming treatment was initiated, six of the 12 WTCs were chosen for isotopic labelling (n = 3 for each treatment), and two additional WTCs were included as unlabelled controls. At the time of labelling, warmed trees (height 6.9 m ± 0.2 SD) were larger than ambient trees (height 5.6 m ± 0.5 SD). On the afternoon of August 5, 2016, the air intake and outlet of the WTCs were sealed to create a well-mixed closed volume, and approximately 1 L of 98% atom percent ^{13}C-CO_2 was injected twice into the aboveground division of each WTC. The first injection occurred at ~1:00 p.m., and the second injection occurred at ~2:00 p.m.

The second injection resulted in isotopic compositions between +7,000‰ and +10,000‰. The $\delta^{13}C$ value of WTC air was monitored by sampling air from each chamber seven times during the labelling event. Chamber air was collected in Tedlar bags and analysed on a cavity ring-down spectroscopy analyser (G2291i; Picarro, Santa Clara, CA). After 4 hr, the WTCs were vented with outside air.

2.3 | Sampling

During the pulse-chase period, various organs were sampled for the measurement of sugar concentrations as well as the $\delta^{13}C$ of sugars and bulk tissues. Leaves were sampled 4, 17, 26, 49, and 438 hr after labelling; phloem was sampled 23, 47, and 167 hr after labelling; and roots were sampled 22, 47, 164, and 621 hr after labelling. Sampling times were chosen to best capture the expected fast turnover of recent photoassimilates in leaves compared to other organs (Epron et al., 2012). Samples were also collected from two unlabelled WTCs throughout the pulse-chase period, as well as from experimental WTCs prior to labelling, to represent the natural C isotope abundance under ambient and warmed conditions.

At each respective sampling time point, two sunlit leaves were collected from the upper one third of the canopy. Phloem samples were collected at approximately 12:00 p.m. A 6 mm × 18 mm cut was initially made using a chisel 1 m from the ground, and each subsequent phloem sample was collected in a zigzag pattern (approximately 4 cm over, 10 cm up). The bark was peeled off and discarded, and the chisel was washed with deionized water between trees. Fine roots (<2 mm diameter) were obtained using a hand trowel (0- to 15-cm depth) and washed with deionized water. All samples were stored at −80°C prior to being freeze-dried and ground for laboratory analyses.

In addition to the measurements that were collected during the pulse-chase period and presented herein (sugar concentrations and $\delta^{13}C$ of sugars and bulk tissues), we also chased the pulse in the respiration of leaves, whole crowns, roots, and soil to quantify the respiratory partitioning of gross primary production and carbon use efficiency (Drake et al., 2019). The $\delta^{13}C$ values of leaf and root respiration during the pulse-labelling period were compared to the $\delta^{13}C$ values of leaf and root sucrose from similar sampling time points to show that sugars were the dominant substrate for respiration (Figure S2; Methods S1). Beginning on November 23, 2016, the trees were fully harvested, and total dry biomass was estimated.

2.4 | Compound-specific and bulk measurement of $\delta^{13}C$ values, and sugar concentrations

To determine the $\delta^{13}C$ and concentration of soluble sugars (raffinose, sucrose, fructose, and glucose), compound-specific isotope analysis was conducted on sugar extracts. Sugars were extracted with 1.0 ml of deionized water per 30 mg of freeze-dried and ground plant material at 85°C for 30 min. After centrifugation, the supernatant was passed over two ion-exchange cartridges (OnGuard II H and OnGuard II A, 1 cc cartridges; Dionex Corporation, Sunnyvale, CA, USA) to remove ionic compounds, and the resulting neutral fraction was collected and analysed for sugars. Compound-specific isotope signatures were measured using a high-performance liquid chromatography system linked to a Delta V Advantage IRMS via a LC IsoLink (both Thermo Electron, Vienna Austria). Sugars were separated on a Nucleogel Pb column (7.8 mm × 300 mm; Machery-Nagel, Germany) with 0.35 ml/min ultrapure water as eluent at 80°C. Sodium persulfate (0.5 M) and phosphoric acid (1.7 M) were used at flow rates of 0.05 ml/min each for the online digestion of the sugars at 100°C in the Isolink device (for details of the method, including system configuration, oxygen removal, and referencing, see Wild, Wanek, Postl, & Richter, 2010). All samples were also analysed for $\delta^{13}C$ of bulk tissue by elemental analyser-isotope ratio mass spectroscopy (Costech 4010 Elemental Analyzer, Thermo Finnigan Delta Plus XP, Bremen, Germany).

To assess the amount of ^{13}C added by pulse-labelling, the $\delta^{13}C$ of labelled samples was first converted to atom percent ^{13}C:

$$AP = \frac{100}{\frac{1}{\left(\frac{\delta^{13}C}{1000}+1\right) \times ARC}+1}, \quad (1)$$

where AP is the isotopic composition in atom percent, $\delta^{13}C$ is the measured isotopic composition in per mil (‰), and ARC is the absolute $^{13}C/^{12}C$ ratio of Vienna PeeDee Belemnite (0.0111802). An identical set of samples was collected prior to labelling, and the atom percent ^{13}C values of unlabelled samples were subtracted from those of labelled samples to determine ^{13}C excess:

$$^{13}C\ excess = AP_{labeled} - AP_{unlabeled}. \quad (2)$$

2.5 | Estimation of MRTs based on an exponential decay function

MRT of C in individual sugars and bulk tissues was determined by an exponential decay function fitted to the ^{13}C excess data using the nls function in R:

$$N(t) = N_0 * e^{-\lambda t}, \quad (3)$$

where t is the time (in hours) at the measured peak of ^{13}C excess, N_0 is the measured peak of ^{13}C excess, and λ is the decay constant. The peak was identified as the maximum ^{13}C excess value captured following the labelling event, but it is important to note that this maximum may differ from the true peak due to our measurement frequency. We then calculated the MRT as 1/λ. Curves were fitted by organ and sugar type for each tree after the maximum in ^{13}C excess had been reached. If less than three data points remained after the maximum in ^{13}C excess, then a curve was not fitted. Goodness of fit was assessed for each curve by comparing predicted values to measured values using Pearson's correlation, α = 0.05 (all $r \geq 0.93$, $P \leq 0.03$).

2.6 | Statistical analyses

Statistical analyses were performed in R version 3.3.2. Linear mixed-effects (lme) models were fit by maximum likelihood using the lme() function. These models contain fixed effects (specified in parentheses below), individual tree as a random effect, and an interaction term to account for tree biomass (biomass x treatment). When there was no repeated measures component (i.e., sampling time), linear models were fit using the lm() function with one categorical factor (treatment). For significant models, differences between pairs of means were evaluated with Tukey's HSD, $\alpha = 0.05$.

To test for differences in sugar concentrations between trees growing in ambient versus warmed WTCs following pulse-labelling, we used a lme model to analyse sugar concentration among sampling times and treatments for each organ and sugar type (sampling time x treatment). Furthermore, to test for differences in the temporal dynamics of $\delta^{13}C$ between trees growing in ambient and warmed WTCs, we used a lme model to analyse $\delta^{13}C$ values among sampling times and treatments for each organ and sugar type or bulk tissue type (sampling time x treatment). To compare MRTs of C in individual sugars and bulk tissues between trees growing in ambient versus warmed WTCs following pulse-labelling, we used a linear model to analyse MRTs among treatments for each organ and sugar type (treatment x biomass).

3 | RESULTS

3.1 | Concentrations of individual sugars

Warming did not alter sugar concentrations, as individual sugar concentrations in the leaves, phloem, and roots did not significantly differ between ambient and warmed treatments (Table 1; all $P \geq 0.14$). Although not statistically significant, there was a trend towards reduced sugar concentrations with experimental warming depending on sugar type and organ. Averaged across treatments and sampling times following pulse-labelling, leaves had the highest total sugar concentrations (55 mg/g ± 3 SE) followed by phloem (33 mg/g ± 2 SE) and roots (21 mg/g ± 2 SE). Sucrose comprised the largest fraction of total sugar concentrations, accounting for approximately 53% (±2 SE) in leaves, 65% (±2 SE) in phloem, and 52% (±3 SE) in roots. In the leaves and roots, fructose was the second largest fraction, accounting for nearly 30%. Interestingly, raffinose made up 26% (±2 SE) of the sugars in the phloem but only 10% (±0.5 SE) and 8% (±0.6 SE) in leaves and roots, respectively.

3.2 | Temporal dynamics of $\delta^{13}C$ throughout whole-trees

Overall, trees dynamically allocated ^{13}C-labelled sugars throughout the aboveground-belowground continuum. Following pulse-labelling, ^{13}C enrichment was highest in the individual sugars and bulk tissue of leaves and decreased when moving vertically down the tree from the leaves to the phloem to the roots. Across organs, peak $\delta^{13}C$ values were generally followed by an exponential decrease, but the time for depletion of the pools back to pre-labelling values increased when moving vertically down the tree. Importantly, the temporal dynamics of $\delta^{13}C$ did not significantly differ between ambient and warmed treatments (all $P \geq 0.09$; Figures 2–5). A summary of these dynamics is provided in Table S1.

At the canopy level, $\delta^{13}C$ values of leaf sugars peaked in the first leaf sampling, which was 4 hr after pulse-labelling (Figure 2). Raffinose (1,150‰ ± 62 SE) and sucrose (852‰ ± 53 SE) were the most highly labelled sugars in the leaves, with $\delta^{13}C$ values that were nearly two times larger than that of fructose and glucose. In line with expected fast MRTs of C in leaf sugars, the ^{13}C label decreased rapidly and was already near natural abundance values 2 days post-labelling.

TABLE 1 Mean concentrations of sugars extracted from leaves, phloem, and roots of *E. parramattensis* growing under ambient and warmed treatments

		Ambient		Warmed	
Tissue	Compound	Conc (mg/g)[a]	SE	Conc (mg/g)[a]	SE
Leaves	Sucrose	33.8	4.3	26.2	2.4
	Glucose	5.9	0.4	4.4	0.3
	Fructose	15.3	0.8	11.8	0.5
	Raffinose	6.1	0.1	5.6	0.2
Phloem	Sucrose	20.4	2.9	22.7	1.4
	Glucose	1.9	0.9	0.9	0.2
	Fructose	2.8	0.4	1.8	0.2
	Raffinose	7.6	0.6	9.0	0.7
Roots	Sucrose	10.3	1.5	11.0	1.8
	Glucose	2.8	0.4	2.3	0.2
	Fructose	8.1	1.5	4.8	0.5
	Raffinose	1.5	0.1	1.5	0.2

[a]Mean ± SE for three trees per treatment across sampling times following pulse-labelling in August 2016. In some cases, sugar concentrations from fewer than three trees were available for a given sampling time. No significant treatment effects were found in linear mixed-effects model testing (all $P \geq 0.14$).

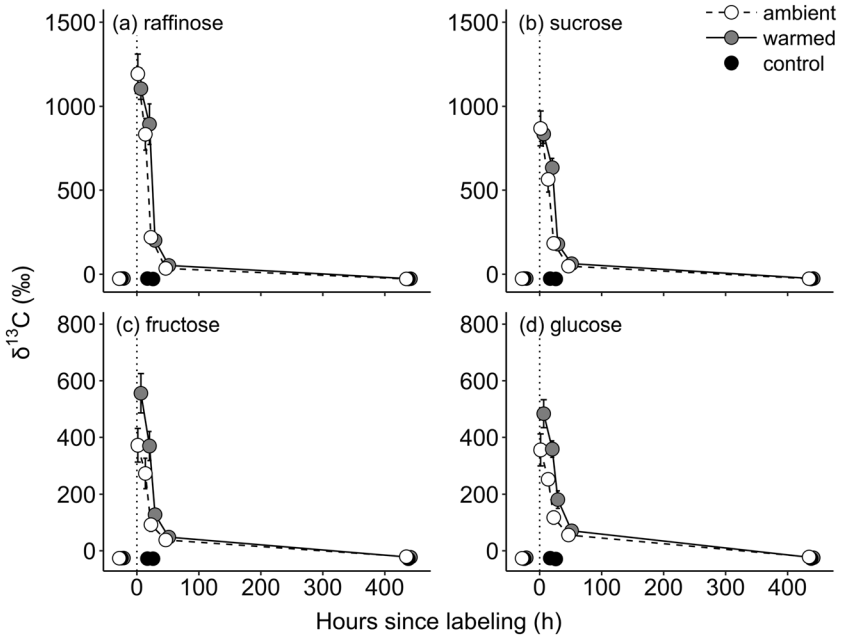

FIGURE 2 Temporal dynamics of the ^{13}C label in leaf (a) raffinose, (b) sucrose, (c) fructose, and (d) glucose for different treatments (ambient, open circles; warmed, grey; and control, black). Error bars denote ± SE of the mean. Mean for three trees per treatment and two control trees at each sampling time. In some cases, the error is smaller than the size of the symbol. Note the difference in *y*-axis scale between plots. Vertical dotted line indicates the labelling event

Similarly, $\delta^{13}C$ values of phloem sugars peaked in the first phloem sampling nearly 24 hr after pulse-labelling but were generally lower than the values observed in the leaves (Figure 3). In both the leaves and the phloem, raffinose was the most highly labelled sugar. Phloem raffinose (865‰ ± 55 SE) was twice as enriched as sucrose (493‰ ± 28 SE). Whereas the ^{13}C label in sugars quickly decreased in the leaves, depletion back to natural abundance values was 3.5 times slower in the phloem.

In the roots, peak $\delta^{13}C$ values were also generally observed during the first root sampling, ranging between 22 and 47 hr, and $\delta^{13}C$ values were generally lower than the values observed in both the leaves and phloem (Figure 4). Raffinose was also the most highly labelled sugar in the roots. While the maximum $\delta^{13}C$ of root raffinose (926‰ ± 86 SE) was in line with that observed in the leaves and phloem, enrichment of the other root sugars was substantially less than in aboveground organs. For example, the maximum $\delta^{13}C$ of sucrose decreased each time by approximately 50% when moving sequentially from the leaves to the phloem to the roots (Figures 2b, 3b, and 4b).

Despite higher enrichment of individual sugars than bulk tissues, our bulk tissue $\delta^{13}C$ results suggest that turnover rates in leaves were remarkably rapid compared to the phloem and roots and newly fixed photoassimilates were contributing less to biomass synthesis in the leaves (Figure 5). In agreement with leaf sugars, the ^{13}C label in bulk leaf tissue peaked 4 hr after pulse-labelling and quickly returned close to pre-labelling $\delta^{13}C$ values within 2 days. The $\delta^{13}C$ dynamics of bulk phloem and phloem sugars were also in agreement with each other. However, in both aboveground organs, a bit of remnant ^{13}C label was still present at the last sampling time point (Figures 5a and 5b). In contrast, a substantial amount of ^{13}C label remained in the roots. While the ^{13}C label in root sugars decreased after 1 week (Figure 4), the ^{13}C label in bulk root tissue remained elevated for nearly 1 month and did not begin to decrease within the time frame of our study (Figure 5c). Thus, we were unable to calculate MRTs for bulk root tissue.

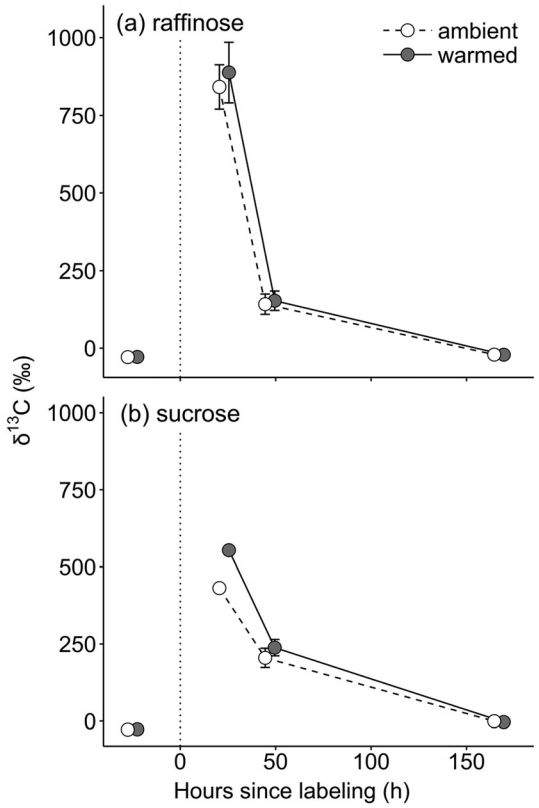

FIGURE 3 Temporal dynamics of the ^{13}C label in phloem (a) raffinose and (b) sucrose for different treatments (ambient, open circles; warmed, grey). Error bars denote ± SE of the mean. Mean for three trees per treatment at each sampling time. In some cases, the error is smaller than the size of the symbol. Vertical dotted line indicates the labelling event

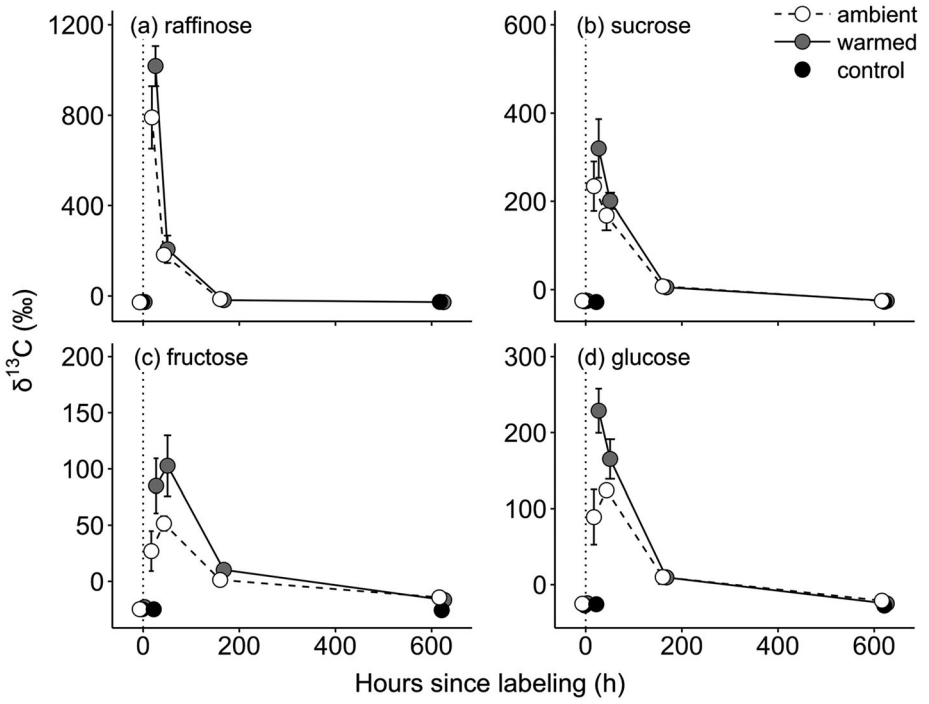

FIGURE 4 Temporal dynamics of the ^{13}C label in root (a) raffinose, (b) sucrose, (c) fructose, and (d) glucose for different treatments (ambient, open circles; warmed, grey; and control, black). Error bars denote ± SE of the mean. Mean for three trees per treatment and two control trees at each sampling time. $\delta^{13}C$ values from fewer trees were available for certain sampling times and treatments in (a) and (d). In some cases, the error is smaller than the size of the symbol. Note the difference in *y*-axis scale between plots. Vertical dotted line indicates the labelling event

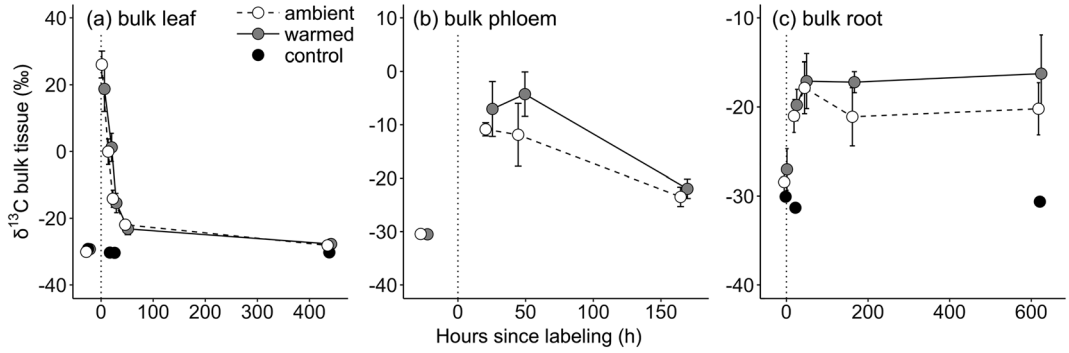

FIGURE 5 Temporal dynamics of the ^{13}C label in bulk tissue of (a) leaves, (b) phloem, and (c) roots for different treatments (ambient, open circles; warmed, grey; and control, black). Error bars denote ± SE of the mean. Mean for three trees per treatment and two control trees at each sampling time. $\delta^{13}C$ values from two ambient trees and one control tree were available for the first sampling time in (c). In some cases, the error is smaller than the size of the symbol. Note the difference in *y*-axis scale between plots. Vertical dotted line indicates the labelling event

3.3 | MRTs of C in individual sugars and bulk tissues

Following ^{13}C-CO_2 application, $\delta^{13}C$ values of sugars spiked and then declined exponentially, such that Equation (3) could be used to estimate MRTs. Warming did not alter the speed of C dynamics, as the MRTs of C in individual sugars in the leaves, phloem, and roots did not significantly differ between ambient and warmed treatments (Table 2; all $P \geq 0.37$). Averaged across treatments following pulse-labelling, sucrose and raffinose had the shortest MRTs for each organ. However, MRTs differed between organs. Our results generally showed increased MRTs of C in sugars moving from the canopy to the root system. For instance, the turnover rate of C in sucrose was faster in the leaves (21 hr ± 1 SE) than in the phloem (35 hr ± 4 SE) and roots (65 hr ± 8 SE).

Similarly, warming did not alter the MRT of C in bulk leaf tissue (P = 0.46; Table 2). Averaged across treatments following pulse-labelling, the MRT of newly fixed C in bulk leaf tissue was 20 hr (±1 SE). This turnover rate was in line with rates for individual leaf sugars. For phloem and roots, there were not enough data points to fit curves; thus, MRTs of C in bulk phloem and root tissues could not be resolved. However, important differences in the temporal dynamics of the ^{13}C label in these bulk tissues were shown in the previous section.

TABLE 2 MRT of C in different compounds/fractions of *E. parramattensis* growing under ambient and warmed treatments

		Ambient		Warmed	
Tissue	Compound	MRT (hr)[a]	SE	MRT (hr)[a]	SE
Leaves	Sucrose	20	1	22	3
	Glucose	28	2	29	4
	Fructose	24	1	22	1
	Raffinose	19	0	18	1
	Bulk	19	2	22	1
Phloem	Sucrose	37	7	32	5
	Raffinose	15	1	15	1
Roots	Sucrose	65	5	66	17
	Glucose	88	6	81	5
	Fructose	158	75	104	30
	Raffinose	19	NA	18	2

Note. MRT, Mean residence time; NA, not applicable.

[a]Mean ± SE of three trees per treatment following pulse labelling in August 2016. MRTs were estimated by fitting an exponential decay function to the observed decline in atom percent ^{13}C excess after pulse-labelling. In some cases, MRTs could only be estimated for one or two trees due to less than three data points for curve fitting (SE). No significant treatment effects were found (all $P \geq 0.37$).

4 | DISCUSSION

4.1 | Experimental warming did not alter C dynamics

Warming was expected to increase carbohydrate utilization and transport, leading to a reduction in the concentrations and MRTs of sugars throughout the trees. However, we observed concentrations and MRTs of sugars that were not reduced under warming. These results suggest that (a) warming of +3°C was insufficient to stimulate carbohydrate utilization and phloem transport, (b) other resources (i.e., water, light, and nutrients) limited stimulation, or (c) the trees physiologically adjusted to the 9-month warming treatment. Previous warming experiments with other *Eucalyptus* species, including a previous experiment in these chambers, lend support for (c) due to their documented strong and nearly homeostatic acclimation of autotrophic respiration to warming (Aspinwall et al., 2016; Drake et al., 2015, 2016).

In this study, complementary measurements taken during the pulse-chase period also showed homeostatic respiratory acclimation of foliar and whole-crown respiration rates and revealed that experimental warming had no impact on respiratory partitioning (Drake et al., 2019). This provides further support for our results, which suggest that *E. parramattensis* was able to adjust its physiology to +3°C as indicated by similar C dynamics between ambient and warmed treatments. Despite that carbon dynamics were not altered under experimental warming, our findings provide insight into the dynamic allocation of ^{13}C-labelled sugars throughout large, field-grown trees.

4.2 | Tracing ^{13}C-labelled sugars throughout whole-trees

In general, pulse-labelling of whole trees revealed that ^{13}C enrichment decreased and MRTs increased moving from the leaves to the phloem to the roots. Trees in our study were taller than 5 m, and it took ^{13}C-labelled sugars approximately 22 hr to travel from the leaves to the roots, implying a transport velocity of 0.28 ± 0.04 m/hr, which is within the 0.20 to 0.82 m/hr range previously reported for eucalypts (Epron et al., 2015). This velocity is likely an underestimate, given that the ^{13}C label was detected in the roots at the first root sampling and its initial presence may have occurred earlier. However, a decrease in the ^{13}C label and increased MRTs when traveling from the canopy to the root system indicate dilution and mixing of ^{13}C-labelled sugars with older unlabelled reserves along the long-distance transport pathway (Furze et al., 2018).

In the leaves, pulse-labelling resulted in maximum $\delta^{13}C$ values of +1,150‰. Leaf sugars in our study represented newly fixed photoassimilates, and a fast decrease in $\delta^{13}C$ values for both leaf sugars and bulk tissue indicated that the sugars were rapidly exported from the leaves, used as substrates for respiration, and/or rapidly diluted by subsequent photoassimilates. In particular, sucrose and raffinose were the most highly labelled sugars and had the fastest turnover rates not only in the leaves, but also across all organs. In previous work, sucrose was identified as having the lowest dilution with older reserves (Streit et al., 2013), and our results suggest that both sucrose and raffinose had lower dilution with unlabelled reserves than other sugars, reflecting their role as transport sugars (Hartmann & Trumbore, 2016). In addition, high enrichment in sucrose and raffinose may reflect not only transport but also storage. These sugars may be stored away in vacuoles, contributing to less exchange with unlabelled reserves.

Although the $\delta^{13}C$ of starch was not quantified in our study, if ^{13}C-labelled starch accumulated in the leaves and was subsequently hydrolyzed into sugars for distribution throughout the trees, these dynamics were accounted for in our $\delta^{13}C$ sugar measurements. While the remnant ^{13}C label present in bulk leaf tissue at the last sampling time point may represent starch storage or incorporation into leaf biomass, our results suggest that the majority of the ^{13}C label was quickly exported or respired from the leaves in sugars. As previous labelling

studies have indicated a close association between starch and sucrose based on similar MRTs for these compounds (Streit et al., 2013), any buildup of ^{13}C-labelled starch in the leaves would likely be transient in nature.

In contrast to aboveground organs, sugars in the root system were the least enriched and had the slowest turnover rates due to mixing with older reserves along the transport pathway. However, whereas the peak in δ^{13}C of root sugars returned to natural abundance after 1 week, the ^{13}C label remained in the bulk root tissue and did not deplete within the month-long time frame of our study. Elevated and persistent δ^{13}C values in bulk root tissue may highlight starch's role as a long-term storage compound in the root system compared to its more transient role in leaves (Barthel et al., 2011; Blessing et al., 2015; Smith & Stitt, 2007). Additionally, persistent enrichment in bulk root tissue may reflect the allocation of newly fixed photoassimilates to root biomass during the pulse-chase period.

4.3 | Phloem loading strategy may influence C dynamics

The whole-tree distribution of photoassimilates discussed above begins in the leaves where sucrose is exported from photosynthetic mesophyll cells into the minor vein phloem. While the mechanism of phloem loading has only been characterized for a few plant species, most passive loaders are thought to be trees (Rennie & Turgeon, 2009; Savage et al., 2017). However, previous work provided evidence for an active polymer trap mechanism in *E. globulus* trees due to the presence of raffinose in phloem sap (Merchant et al., 2010); we also found this in our study species *E. parramattensis*. During polymer trapping, sucrose in the leaf mesophyll diffuses into specialized companion cells in the minor vein. There, sucrose is converted into larger oligosaccharides like raffinose and stachyose that cannot back diffuse, and thus, these compounds accumulate in the phloem (Turgeon, 2010; Figure 1a).

The impact of environmental factors on phloem physiology, including phloem loading at the leaf-level and phloem physiology along the transport pathway, is not well understood in field-grown trees (Ayre, 2011; Van Bel, 2003; Xu, Chen, Ren, Chen, & Liesche, 2018), but loading strategy has potential implications for whole-tree C relations. Given that polymer trapping is an active phloem loading mechanism (Turgeon, 2010), we hypothesize that it may enable polymer trapping species to have tighter regulation of C export at the leaf mesophyll-phloem interface and in turn make C allocation less sensitive to changes in environmental factors like temperature, light, and CO_2. Although it remains unclear if loading strategy is phylogenetically conserved (Davidson, Keller, & Turgeon, 2011; Gamalei, 1989; Turgeon, Medville, & Nixon, 2001), other eucalypt species may respond similarly to environmental perturbations. While our results provide evidence for this mechanism in *E. parramattensis*, future studies should couple the exposure of leaves to exogenous labelled sugars with spatially explicit isotope analysis (such as autoradiography or secondary ion mass spectrometry (SIMS) to confirm phloem loading strategy (Rennie & Turgeon, 2009).

4.4 | CONCLUSIONS

Combining long-term experimental warming along with ^{13}C-CO_2 pulse-labelling and compound-specific isotope analysis to trace recently assimilated sugars from the leaves to the roots of large whole-trees in the field provided insights into the C source-sink relations of *E. parramattensis*, but did not reveal an effect of temperature on these dynamics. While ^{13}C-labelled sugars were dynamically allocated throughout the trees, less enrichment and longer MRTs in belowground compared to aboveground organs indicated that the ^{13}C-labelled sugars were diluted by unlabelled reserves as well as with distance from the source along the transport pathway. Further, the presence of raffinose in the phloem provided evidence for a polymer trap mechanism for phloem loading, which may contribute to eucalypt species' ability to counter stressors associated with global change. Thus, our results improve understanding of C dynamics at the whole-tree level and, importantly, provide insight into the physiological and environmental controls on within-tree C relations.

ACKNOWLEDGEMENTS

This work was supported by the National Science Foundation's Inter-University Training for Continental Scale Ecology programme (Grant 1137336), the National Science Foundation's Graduate Research Fellowship programme (Grant DGE1144152), and the National Science Foundation's Graduate Research Opportunities Worldwide programme. We thank Mark Tjoelker and Craig Barton for their coordination and maintenance of the WTC study as well as Angelica Vårhammer, Dushan Kumarathunge, and Anne Griebel for their help with sample collection. We also thank Molly Wieringa and Elizabeth Rao for their help with data entry and sample preparation, Jessica Gersony and Missy Holbrook for their knowledge on phloem physiology, the Richardson laboratory for use of their laboratory space and equipment, and the University of Wyoming Stable Isotope Facility for conducting bulk stable isotope analysis. Additionally, M.E.F., J.E.D., and E.P. thank the Hawkesbury Institute for the Environment's Research-in-Residence programme and the University of Utah's IsoCamp for their generous support of this work. The WTC experiment was made possible through a collaboration with Sune Linder and the Swedish University of Agricultural Sciences, who designed, built, and provided the whole tree chambers. The WTC experiment was supported by the Australian Research Council (Discovery, DP140103415), a New South Wales government Climate Action Grant (NSW T07/CAG/016), the Hawkesbury Institute for the Environment, and Western Sydney University.

CONFLICT OF INTEREST

The authors declare that there is no conflict of interest.

ORCID

Morgan E. Furze https://orcid.org/0000-0001-9690-6218

REFERENCES

Aspinwall, M. J., Drake, J. E., Campany, C., Vårhammar, A., Ghannoum, O., Tissue, D. T., … Tjoelker, M. G. (2016). Convergent acclimation of leaf photosynthesis and respiration to prevailing ambient temperatures under current and warmer climates in *Eucalyptus tereticornis*. *New Phytologist*, *212*, 354–367. https://doi.org/10.1111/nph.14035

Atkin, O. K., & Tjoelker, M. G. (2003). Thermal acclimation and the dynamic response of plant respiration to temperature. *Trends in Plant Science*, *8*, 343–351. https://doi.org/10.1016/S1360-1385(03)00136-5

Australian Bureau of Meteorology State of the Climate Report (2016).

Ayre, B. G. (2011). Membrane-transport systems for sucrose in relation to whole-plant carbon partitioning. *Molecular Plant*, *4*, 377–394. https://doi.org/10.1093/mp/ssr014

Barthel, M., Hammerle, A., Sturm, P., Baur, T., Gentsch, L., & Knohl, A. (2011). The diel imprint of leaf metabolism on the $\delta^{13}C$ signal of soil respiration under control and drought conditions. *New Phytologist*, *192*, 925–938. https://doi.org/10.1111/j.1469-8137.2011.03848.x

Barton, C. V. M., Ellsworth, D. S., Medlyn, B. E., Duursma, R. A., Tissue, D. T., Adams, M. A., … Linder, S. (2010). Whole-tree chambers for elevated atmospheric CO_2 experimentation and tree scale flux measurements in south-eastern Australia: The Hawkesbury Forest Experiment. *Agricultural and Forest Meteorology*, *150*, 941–951. https://doi.org/10.1016/j.agrformet.2010.03.001

Blessing, C. H., Werner, R. A., Siegwolf, R., & Buchmann, N. (2015). Allocation dynamics of recently fixed carbon in beech saplings in response to increased temperatures and drought. *Tree Physiology*, *35*, 585–598. https://doi.org/10.1093/treephys/tpv024

Dannoura, M., Maillard, P., Fresneau, C., Plain, C., Berveiller, D., Damesin, C., … Epron, D. (2011). *In situ* assessment of the velocity of carbon transfer by tracing ^{13}C in trunk CO_2 efflux after pulse labelling: Variations among tree species and seasons. *New Phytologist*, *190*, 181–192. https://doi.org/10.1111/j.1469-8137.2010.03599.x

Davidson, A., Keller, F., & Turgeon, R. (2011). Phloem loading, plant growth form, and climate. *Protoplasma*, *248*, 153–163. https://doi.org/10.1007/s00709-010-0240-7

Drake, J. E., Aspinwall, M. J., Pfautsch, S., Rymer, P. D., Reich, P. B., Smith, R. A., … Tjoelker, M. G. (2015). The capacity to cope with climate warming declines from temperate to tropical latitudes in two widely distributed *Eucalyptus* species. *Global Change Biology*, *21*, 459–472. https://doi.org/10.1111/gcb.12729

Drake, J. E., Furze, M. E., Tjoelker, M. G., Carrillo, Y., Barton, C. V. M., & Pendall, E. (2019). Climate warming and tree carbon use efficiency in a whole-tree $^{13}CO_2$ tracer study. *New Phytologist*, *222*, 1313–1324. https://doi.org/10.1111/nph.15721

Drake, J. E., Tjoelker, M. G., Aspinwall, M. J., Reich, P. B., Barton, C. V. M., Medlyn, B. E., & Duursma, R. A. (2016). Does physiological acclimation to climate warming stabilize the ratio of canopy respiration to photosynthesis? *New Phytologist*, *211*, 850–863. https://doi.org/10.1111/nph.13978

Drake, J. E., Tjoelker, M. G., Vårhammar, A., Medlyn, B. E., Reich, P. B., Leigh, A., … Barton, C. V. M. (2018). Trees tolerate an extreme heatwave via sustained transpirational cooling and increased leaf thermal tolerance. *Global Change Biology*, *24*, 2390–2402. https://doi.org/10.1111/gcb.14037

Duursma, R. A., & Falster, D. S. (2016). Leaf mass per area, not total leaf area, drives differences in above-ground biomass distribution among woody plant functional types. *New Phytologist*, *212*, 368–376. https://doi.org/10.1111/nph.14033

Endrulat, T., Saurer, M., Buchmann, N., & Brunner, I. (2010). Incorporation and remobilization of ^{13}C within the fine-root systems of individual *Abies alba* trees in a temperate coniferous stand. *Tree Physiology*, *30*, 1515–1527. https://doi.org/10.1093/treephys/tpq090

Epron, D., Bahn, M., Derrien, D., Lattanzi, F. A., Pumpanen, J., Gessler, A., … Buchmann, N. (2012). Pulse-labelling trees to study carbon allocation dynamics: A review of methods, current knowledge and future prospects. *Tree Physiology*, *32*, 776–798. https://doi.org/10.1093/treephys/tps057

Epron, D., Cabral, O. M. R., Laclau, J. P., Dannoura, M., Packer, A. P., Plain, C., … Nouvellon, Y. (2015). In situ $^{13}CO_2$ pulse labelling of field-grown eucalypt trees revealed the effects of potassium nutrition and throughfall exclusion on phloem transport of photosynthetic carbon. *Tree Physiology*, *36*, 6–21.

Epron, D., Ngao, J., Dannoura, M., Bakker, M. R., Zeller, B., Bazot, S., … Loustau, D. (2011). Seasonal variations of belowground carbon transfer assessed by in situ $^{13}CO_2$ pulse labelling of trees. *Biogeosciences*, *8*, 1153–1168. https://doi.org/10.5194/bg-8-1153-2011

Furze, M. E., Trumbore, S., & Hartmann, H. (2018). Detours on the phloem sugar highway: Stem carbon storage and remobilization. *Current Opinion in Plant Biology*, *43*, 89–95. https://doi.org/10.1016/j.pbi.2018.02.005

Gamalei, Y. (1989). Structure and function of leaf minor veings in trees and herbs. *Trees*, *3*, 96–110. https://doi.org/10.1007/BF01021073

Hartmann, H., & Trumbore, S. (2016). Understanding the roles of nonstructural carbohydrates in forest trees—From what we can measure to what we want to know. *New Phytologist*, *211*, 386–403. https://doi.org/10.1111/nph.13955

Hesse, B. D., Goisser, M., Hartmann, H., & Grams, T. E. E. (2018). Repeated summer drought delays sugar export from the leaf and impairs phloem transport in mature beech. *Tree Physiology*, *39*, 1–9.

IPCC (2014). *Climate change 2014: Synthesis report*. Geneva, Switzerland: IPCC.

Kagawa, A., Sugimoto, A., & Maximov, T. C. (2006a). Seasonal course of translocation, storage and remobilization of 13C pulse-labeled photoassimilate in naturally growing Larix gmelinii saplings. *New Phytologist*, *171*, 793–803. https://doi.org/10.1111/j.1469-8137.2006.01780.x

Kagawa, A., Sugimoto, A., & Maximov, T. C. (2006b). $^{13}CO_2$ pulse-labelling of photoassimilates reveals carbon allocation within and between tree rings. *Plant, Cell and Environment*, *29*, 1571–1584. https://doi.org/10.1111/j.1365-3040.2006.01533.x

Keel, S. G., Campbell, C. D., Högberg, M. N., Richter, A., Wild, B., Zhou, X., … Högberg, P. (2012). Allocation of carbon to fine root compounds and their residence times in a boreal forest depend on root size class and season. *New Phytologist*, *194*, 972–981. https://doi.org/10.1111/j.1469-8137.2012.04120.x

Knoblauch, M., Knoblauch, J., Mullendore, D. L., Savage, J. A., Babst, B. A., Beecher, S. D., … Holbrook, N. M. (2016). Testing the Münch hypothesis of long distance phloem transport in plants. *eLife*, *5*, 1–16.

Kozlowski, T. T. (1992). Carbohydrate sources and sinks in woody plants. *Botanical Review*, *58*, 107–222. https://doi.org/10.1007/BF02858600

Kuptz, D., Fleischmann, F., Matyssek, R., & Grams, T. E. E. (2011). Seasonal patterns of carbon allocation to respiratory pools in 60-yr-old deciduous (*Fagus sylvatica*) and evergreen (*Picea abies*) trees assessed via whole-tree stable carbon isotope labeling. *New Phytologist*, *191*, 160–172. https://doi.org/10.1111/j.1469-8137.2011.03676.x

Merchant, A., Peuke, A. D., Keitel, C., MacFarlane, C., Warren, C. R., & Adams, M. A. (2010). Phloem sap and leaf $\delta^{13}C$, carbohydrates, and amino acid concentrations in *Eucalyptus globulus* change systematically according to flooding and water deficit treatment. *Journal of Experimental Botany*, *61*, 1785–1793. https://doi.org/10.1093/jxb/erq045

Münch, E. (1930). *Die Stoffbewegungen in der Pflanze*. Jena, Germany: Gustav Fischer Verlagsbücher.

Plain, C., Gerant, D., Maillard, P., Dannoura, M., Dong, Y., Zeller, B., … Epron, D. (2009). Tracing of recently assimilated carbon in respiration at high temporal resolution in the field with a tuneable diode laser absorption spectrometer after *in situ* $^{13}CO_2$ pulse labelling of 20-year-old beech trees. *Tree Physiology*, *29*, 1433–1445. https://doi.org/10.1093/treephys/tpp072

Poorter, H., Niklas, K. J., Reich, P. B., Oleksyn, J., Poot, P., & Mommer, L. (2012). Biomass allocation to leaves, stems and roots: Meta-analyses of interspecific variation and environmental control. *New Phytologist*, *193*, 30–50. https://doi.org/10.1111/j.1469-8137.2011.03952.x

Reich, P. B., Sendall, K. M., Stefanski, A., Wei, X., Rich, R. L., & Montgomery, R. A. (2016). Boreal and temperate trees show strong acclimation of respiration to warming. *Nature*, *531*, 633–636. https://doi.org/10.1038/nature17142

Rennie, E. A., & Turgeon, R. (2009). A comprehensive picture of phloem loading strategies. *Proceedings of the National Academy of Sciences*, *106*, 14162–14167. https://doi.org/10.1073/pnas.0902279106

Richter, A., Wanek, W., Werner, R. A., Ghashghaie, J., Gessler, A., Brugnoli, E., … So, K. (2009). Preparation of starch and soluble sugars of plant material for the analysis of carbon isotope composition: a comparison of methods. *Rapid Communications in Mass Spectrometry*, *23*, 2476–2488. https://doi.org/10.1002/rcm.4088

Savage, J. A., Beecher, S. D., Clerx, L., Gersony, J. T., Knoblauch, J., Losada, J. M., … Holbrook, N. M. (2017). Maintenance of carbohydrate transport in tall trees. *Nature Plants*, *3*, 965–972. https://doi.org/10.1038/s41477-017-0064-y

Slot, M., & Kitajima, K. (2015). General patterns of acclimation of leaf respiration to elevated temperatures across biomes and plant types. *Oecologia*, *177*, 885–900. https://doi.org/10.1007/s00442-014-3159-4

Smith, A. M., & Stitt, M. (2007). Coordination of carbon supply and plant growth. *Plant, Cell & Environment*, *30*, 1126–1149. https://doi.org/10.1111/j.1365-3040.2007.01708.x

Streit, K., Rinne, K. T., Hagedorn, F., Dawes, M. A., Saurer, M., Hoch, G., … Siegwolf, R. T. W. (2013). Tracing fresh assimilates through *Larix decidua* exposed to elevated CO and soil warming at the alpine treeline using compound-specific stable isotope analysis. *New Phytologist*, *197*, 838–849. https://doi.org/10.1111/nph.12074

Turgeon, R. (2010). The role of phloem loading reconsidered. *Plant Physiology*, *152*, 1817–1823. https://doi.org/10.1104/pp.110.153023

Turgeon, R., Medville, R., & Nixon, K. (2001). The evolution of minor vein phloem and phloem loading. *American Journal of Botany*, *88*, 1331–1339. https://doi.org/10.2307/3558441

Van Bel, A. J. E. (2003). The phloem, a miracle of ingenuity. *Plant, Cell and Environment*, *26*, 125–149.

Vizoso, S., Gerant, D., Guehl, J. M., Joffre, R., Charlot, M., Gross, P., & Maillard, P. (2008). Do elevation of CO_2 concentration and nitrogen fertilization after storage and remobilization of carbon and nitrogen in pedunculate oak saplings? *Tree Physiology*, *28*, 1729–1739. https://doi.org/10.1093/treephys/28.11.1729

Warren, J. M., Iversen, C. M., Garten, C. T., Norby, R. J., Childs, J., Brice, D., … Weston, D. J. (2012). Timing and magnitude of C partitioning through a young loblolly pine (*Pinus taeda* L.) stand using ^{13}C labeling and shade treatments. *Tree Physiology*, *32*, 799–813. https://doi.org/10.1093/treephys/tpr129

Wild, B., Wanek, W., Postl, W., & Richter, A. (2010). Contribution of carbon fixed by Rubisco and PEPC to phloem export in the Crassulacean acid metabolism plant *Kalanchoë daigremontiana*. *Journal of Experimental Botany*, *61*, 1375–1383. https://doi.org/10.1093/jxb/erq006

Xu, Q., Chen, S., Ren, Y., Chen, S., & Liesche, J. (2018). Regulation of sucrose transporters and phloem loading in response to environmental cues. *Plant Physiology*, *176*, 930–945. https://doi.org/10.1104/pp.17.01088

Yamori, W., Hikosaka, K., & Way, D. A. (2014). Temperature response of photosynthesis in C3, C4, and CAM plants: Temperature acclimation and temperature adaptation. *Photosynthesis Research*, *119*, 101–117. https://doi.org/10.1007/s11120-013-9874-6

SUPPORTING INFORMATION

Additional supporting information may be found online in the Supporting Information section at the end of the article.

Table S1 Summary of temporal dynamics (mean residence time (MRT; hours), time of peak $\delta^{13}C$ value (hours since labeling), and peak $\delta^{13}C$ value (‰)) for each tree component (leaves, phloem, and roots) and type (sucrose, glucose, fructose, raffinose, and bulk). Data are averaged across ambient and warmed treatments and presented as mean (SE).

Figure S1 Volumetric water content (VWC) of the ambient (blue) and warmed (red) treatments during the pulse-chase period. Several lines of evidence suggest that the trees did not experience biologically meaningful water deficits between waterings. First, volumetric soil water content remained sufficiently high between watering events, declining to only 0.12 m^3m^{-3}, which reflects a high amount of plant available water in this sandy soil (see plot below). Second, the watering regime was designed to provide the trees with sufficient moisture to create a "well-watered" condition. Whole-tree transpiration rates were measured directly with the WTC system, and these fluxes did not vary between watering events. That is, transpiration varied strongly from day to day as a function of temperature, VPD, and light, but fluxes did not decline over time and then increase after watering. Finally, we did measure leaf water potential on September 19th, 2016, which fell in the middle of a two-week watering period. Predawn leaf water potentials averaged −0.22 and − 0.16 MPa in the ambient and warmed treatments, respectively. These values did not differ significantly across treatments ($P > 0.5$)

Figure S2 Comparison of $\delta^{13}C$ of respiration and $\delta^{13}C$ of sucrose in a) leaves and b) roots. Strength of association was evaluated using Pearson's correlation, $\alpha = 0.05$. See Methods S1.

Methods S1 Measurement of $\delta^{13}C$ of respiration in leaves and roots

How to cite this article: Furze ME, Drake JE, Wiesenbauer J, Richter A, Pendall E. Carbon isotopic tracing of sugars throughout whole-trees exposed to climate warming. *Plant Cell Environ*. 2019;1–11. https://doi.org/10.1111/pce.13625